

# Final Report

## Micro-Patterned Membrane Surfaces with Switchable Hydrophobicity

*PIs:* Carl Frick, Department of Mechanical Engineering, University of Wyoming  
Jonathan Brant, Department of Civil Engineering, University of Wyoming

*Dates:* March 1, 2013 – February 28, 2015

### Abstract:

Interest in, and the use of, membrane distillation for desalination applications is growing in areas like Wyoming that are grappling with dwindling freshwater supplies and the large volumes of saline water that are generated from the development of our energy resources. Realizing the full potential of membrane distillation hinges on the development of new membrane materials that are tailored for the unique requirements of this process. The *overarching goal* of this research was the synthesis, characterization, and testing of a preliminary hierarchical membrane surface coating whose properties can be changed in response to environmental stimuli. The *objective* was to create a structured surface capable of switchable hydrophobicity. It was our *central premise* that a biologically inspired patterned surface manufactured through conventional soft molding techniques using shape-memory polymers, will create a highly hydrophobic surface when erect, while demonstrating dramatically less hydrophobicity when in a relaxed state, as a result of the relationship between surface roughness and hydrophobicity. Such a surface would facilitate easier cleaning of the membrane by backwashing, while maximizing the separation efficiency and permeate flux rate through the membrane. Our *rationale* for undertaking this research was that new treatment strategies, like membrane distillation, are needed to effectively manage highly saline waters. We accomplished the overall objective of this proposal by pursuing the following specific aims:

*Specific Aim #1 – Synthesize membrane surface treatments from shape-memory polymers having tunable surface structure controlled hydrophobicity.* Standard soft molding techniques were used to fabricate proof of concept, small-scale pattern, consisting of arrays of vertical micro-pillars. These pillars were supplemented with spatially tailored surface treatments to further enhance the overall switchable wettability effect.

*Specific Aim #2 – Assess and evaluate the efficacy of membrane surfaces with tunable surface structure and hydrophobicity.* We characterized the structure and hydrophobicity of the shape-memory polymer structures as a function of environmental parameters relevant to membrane distillation applications and evaluated any changes in polymer structure in terms of their impact on membrane performance.

## 1 Purpose and Objectives:

The overarching goal of this research was to create a proof-of-concept structured surface that could ultimately be cast onto water filtration membranes out of a unique, multi-tiered platform consisting of a thermo-mechanically tailored polymer understructure arrayed in a pillared pattern that is overlaid with various hydrophobic/hydrophilic surface treatments. It is through the combination of the underlying polymer system, preferential surface treatments, and patterned structure that the effect is believed to assist in the anti-fouling properties and aid in “self-cleaning” during membrane backwashing.

It is our central premise that a biologically inspired micro-patterned surface manufactured through conventional molding techniques using thermo-mechanically tailored acrylate based polymers as well as various surface treatments will assist in antifouling in two ways. First, through a change in wetting characteristics. It is our hypothesis that we could create a highly hydrophobic surface when erect, while demonstrating a dramatically less hydrophobic - even hydrophilic - system when in a relaxed state, as a result of the relationship between surface roughness and surface chemistry. Through this stark change in characteristics, it is possible to deter a wide array of fouling materials based off their specific surface interactions, whether hydrophilic or hydrophobic in nature instead of targeting just one specific group. At the same time, the geometrical structuring of the pillars are expected to continue to allow for water transport across the membrane even in a hydrophobic state because of the expected size scale, allowing for advective transport to the membrane similar to that seen in porous membranes [1].

Second, is through the mechanical alteration of the material properties within the structured surface. Through changing the material from a rigid state to a pliable state with an increase in temperature, it was hypothesized that a buildup of fouling materials will be destabilized and encouraged to break off during the back flushing process, continuing into the waste stream, lowering the amount of irreversible fouling inherent to the pressure driven membrane process. This proposed process can be seen in **Figure 1**.

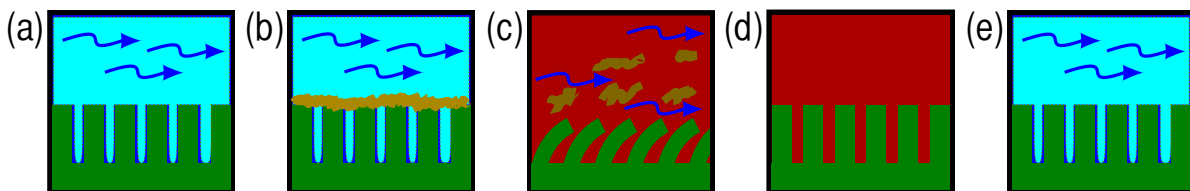


**Figure 1:** Proposed cleaning process and switching between hydrophobic to hydrophilic states on a micro-patterned surface. (a) The structured surface in normal operating conditions. (b) Significant fouling has built up. (c) The pillars become pliable under heating while crossflow continues, encouraging breakoff. (d) Halting of crossflow, and recovery of original shape. (e) Normal operation conditions commence.

In **Figure 1** (a), the structured surface appears in normal operating conditions at low temperatures and hydrophobic state. After significant fouling has built up in (b), the water is heated while the crossflow continues, and the pillars become pliable, switching to a hydrophilic state; encouraging breakoff (c). At the end of the cleaning process crossflow pressure is stopped, allowing the pillars to return to an undeformed state (d). The material is then cooled to a lower temperature for normal operations to resume in (e).

The research performed here lays out the foundation for which future research can build upon, while steps in the future can focus on decreasing the overall size scale, optimizing pattern parameters, and manufacturing techniques to place this on an operating membrane. Our rationale for undertaking this

research is that new treatment strategies, like membrane distillation, are needed to effectively manage highly saline waters. The ultimate goal of the Investigators is to leverage these results towards an SBIR proposal geared toward developing our switchable hydrophobic surfaces for commercial applications.

## **2 Problem:**

Population growth, energy development, and agricultural interests are all competing for the limited freshwater supplies in Rocky Mountain region. As such, both industry and the public sector are using less pristine raw water sources such as brackish groundwater and oil and gas produced waters in an attempt to develop new water supplies [2]. Desalination is therefore receiving serious interest across the western US, for managing produced waters and augmentation of drinking water supplies [3,4]. Membrane fouling owing to high-energy requirements on the part of pressure driven membrane processes however remain significant challenges to processes like reverse osmosis (RO). An important need is the development of a membrane surface coating whose surface structure may be manipulated, i.e., a smart surface, to be rigid during process operation and flexible to facilitate backwashing the membrane during cleaning to optimize permeability recovery. The development of new materials whose surface properties may be controlled so as to provide greater flexibility in process operation is needed to realize the full potential of membrane distillation processes. In the absence of such advancements, the use of membrane distillation in desalination applications will be stagnated, particularly for produced waters, which have high total dissolved solids (salt) concentrations.

## **3 Methodology:**

The research approach for this project could be broken into five major steps. Steps included (1) investigation into fundamental thermo-mechanical observations of nine acryl-based macromolecules (five monofunctional and four multifunctional) chosen from the broad class of acrylate monomers. The nine macromolecules were initially selected based off their expected low toxicity, ability to be polymerized through a chain polymerization process activated by a photoinitiator, and based off a diverse variety of functional groups allowing for a range of wetting characteristics and glass transitions. These select compounds can be seen in **Figure 2**.



would be counterproductive. The final requirement of surface treatments is the ability to preferentially layer the system to enhance the structured surfaces hydrophobic and hydrophilic effects.

Investigation was made through a series of systematic studies incorporating polymer synthesis, various thermo-mechanical tests utilizing Dynamic Mechanical Analysis (DMA) and temperature dependent load frame testing, observation of water absorption characteristics, molding techniques, and various surface characterization techniques.

## 6 Principal Findings:

### 6.1 Base Polymer Networks

Initially, nine acryl based macromolecule systems were investigated both for their thermo-mechanical behavior as well as water absorption in order to ultimately isolate an optimal combination of systems based on aqueous glass transition behavior, water absorption, and mechanical properties. For the proposed application it was determined that the polymer systems must exhibit good shape-memory properties targeted for an onset temperature of approximately 30-40°C under submerged conditions, appropriate high and low temperature mechanical properties including strain-to-failure, and the ability to be photopolymerized into a structured surface. Five of these initial systems were monofunctional (linear-builders), while the remaining four were multifunctional (crosslinking) molecules. To ensure good shape-memory effects, both linear builders, as well as a light amount of crosslinking are necessary. A small amount of crosslinking in the system is added for two reasons: it will allow for hard segments needed for the polymer to remember its initial shape, and to assist in a well-established rubbery regime. However, too much crosslinking and the material ductility will greatly decrease. Additionally, the amount of cross linking is expected to dramatically affect the amount of water absorption due to an alteration in the amount of free volume in the polymer network. The nine macromolecules were chosen from a broad family based on ease of fabrication and nontoxicity.

Water absorption testes were run using ultra-pure water over a duration of 10 days; results can be seen in **Figure 3**. For linear builders, water absorption ranged from  $53.8 \pm 1.2\%$  to  $0.94 \pm 0.47\%$  represented by 2HEMA and tBA. Water absorption for pure crosslinkers ranged from  $44.2 \pm 2.7\%$  to  $3.9 \pm 1.2\%$  as PEGDMA750 and DEGDMA. The water absorption reached steady state for all synthesized polymers within approximately one day. It is worthy of note that 2CEA is not included in the part (a) of the figure as it dissolved in the water within the initial testing period of 1 hour.

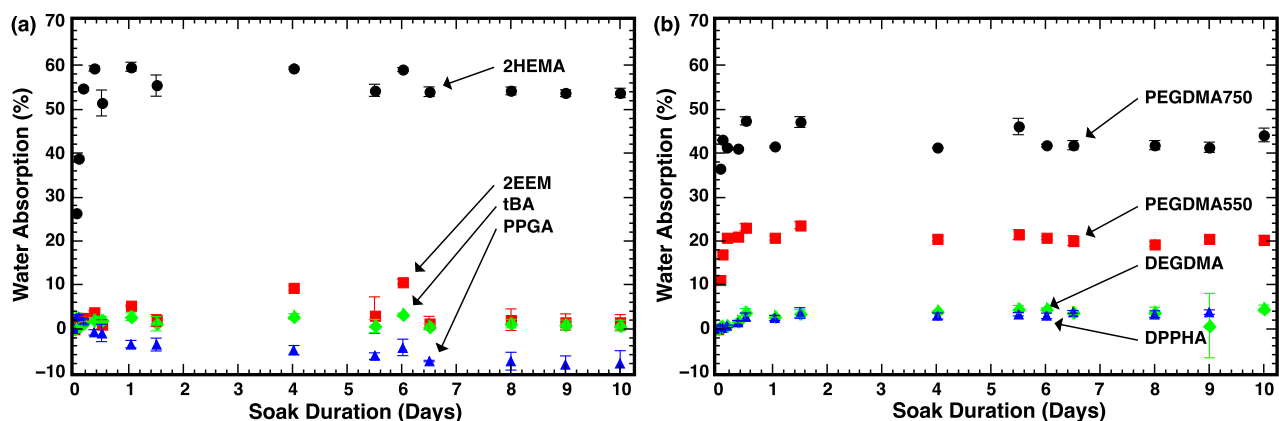


**Figure 3:** Water absorption for individual (a) monofunctional and (b) multifunctional acryl systems. Note 2CEA dissolved in water and therefore has not been included.

Initial thermo-mechanical testing of soaked samples was performed using the DMA to observe each constituents dry glass transition temperature, storage modulus in the rubbery and glassy regime, and shape-memory properties reflected in **Figure 4**. A material is expected to exhibit promising shape-memory effects if there is a large transition in the storage modulus over the transition region, altering the material from a stiff, rigid state to a soft, pliable state as temperature, combine this over a short temperature range and the result is a steep transition region such as the tBA curve of **Figure 4**.

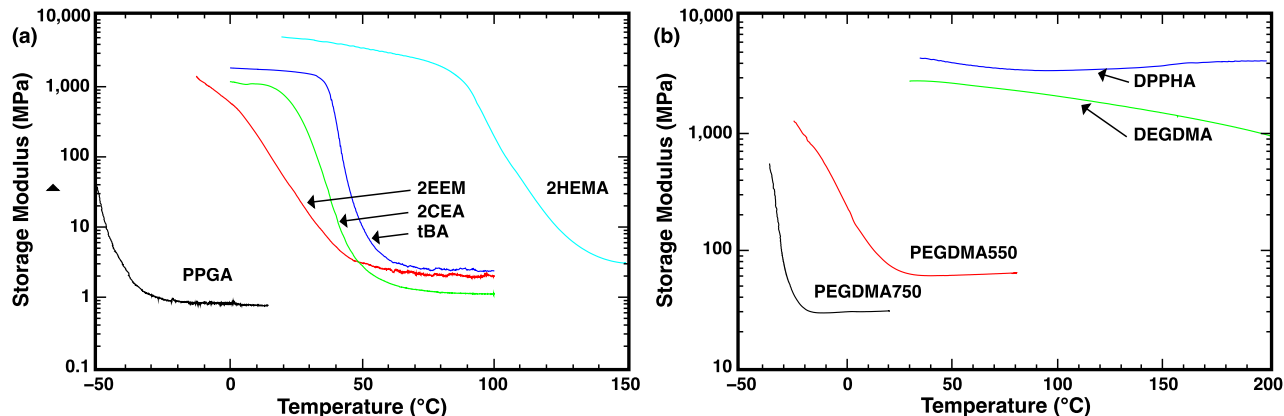


**Figure 4:** Representative curves of storage modulus transition as a function of temperature for individual (a) monofunctional and (b) multifunctional acryl systems. Results obtained from DMA.

## 6.2 Ternary Polymer Networks

Based on the observations in the last section, three polymer constituents were chosen to systematically vary including the linear builders tBA and 2HEMA, along with a small weight percentage of the crosslinker PEGDMA550. The choices of macromolecules were based on water absorption properties and promise of good shape-memory characteristics at the desired onset temperature around 30-45°C when soaked. As aforementioned, a light amount of crosslinking has historically shown better shape-memory effects. Because of this, the weight percentage of PEGDMA500, the crosslinker and DMAPA, the photoinitiator were held constant at 5% and 0.5% of the total respectively, while the relative percentage of tBA to 2HEMA were varied in six sample sets. Note that 2HEMA has a high water absorption at 53.8

$\pm 1.2\%$ , while tBA was much lower  $0.94 \pm 0.47\%$  in **Figure 3**. Therefore through the varying the relative percentage, an alteration in the amount of water absorption is expected. This is reflected in **Figure 5**. In the figure the relative percentage of the 94.5% linear building solution change from 100/0, 90/10, 75/25, 50/50, 25/75, 0/100, tBA to 2HEMA.

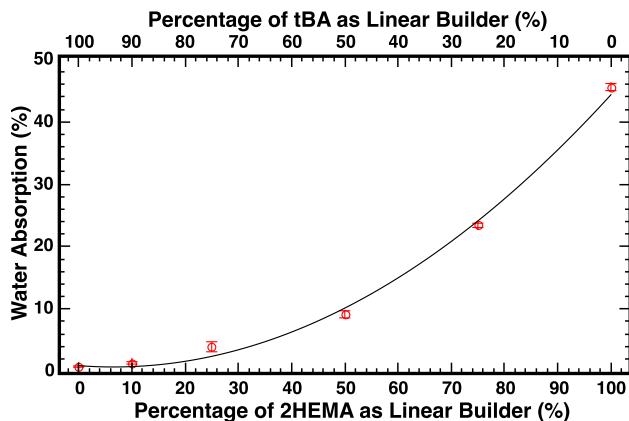


**Figure 5:** Water absorption as a function of varying the relative amounts of tBA and 2HEMA in a system with 5 wt.% PEGDMA550.

As the percentage of 2HEMA in the system increased there was an increase in the water content displayed in the curve fit. The target water absorption of approximately 4% of the materials original mass was a predetermined value.

**Figure 6 (a)** displays representative curves of storage moduli with samples in dry form. The glass moduli of the materials are relatively consistent ranging between 2 and 3 GPa, while the rubbery modulus of the materials range from approximately 1 to 10 MPa. General trends observed as the monofunctional builder mixture transitioned from a low percentage of 2HEMA to a low percentage of tBA is an increase in the glass transition temperature, and a gradual lengthening of the transition region.

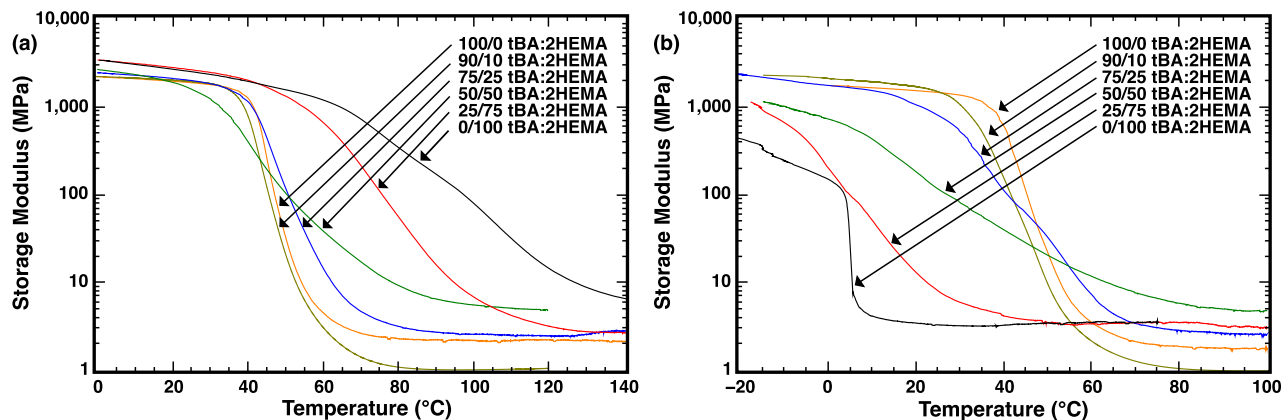


**Figure 6:** Representative (a) dry and (b) soaked DMA tests maintaining 5 wt.% PEGDMA550, while varying the relative wt. ratio of linear builders tBA and 2HEMA.

Similarly **Figure 6 (b)** shows the results of DMA testing for soaked samples. However, as the amount of 2HEMA increases in the linear building mixture now, the glass transition of the material tends to decrease. This is indicative to the amount of water absorbed into the system, as compared to **Figure 5** seen before.

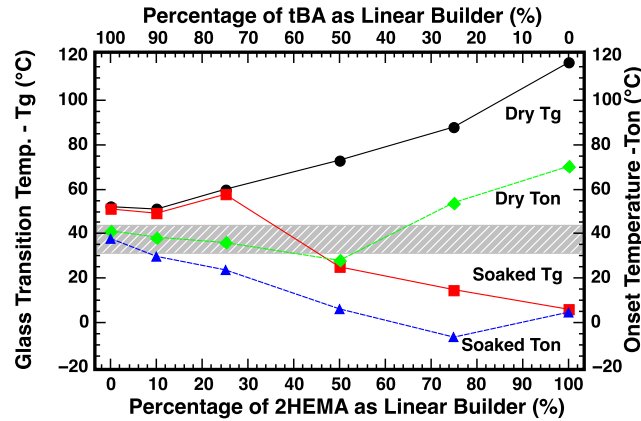


**Figure 7:** Effect on glass transition temperature and onset temperature as a function of varying the relative amounts of tBA and 2HEMA in a system with 5 wt.% PEGDMA550 for both dry and soaked samples.

To clarify results, a trend of both the glass transition temperatures and the onset temperatures of soaked and dry samples are displayed in **Figure 7**. The glass transition temperature is defined here as the peak of the Tan Delta curve, which has been omitted for clarity, and the onset temperature chosen as the intersect of two tangent lines to the glassy and transition regions. Note the target region for the onset of the shape-memory transition is displayed as the hashed gray region between 30°C and 45°C. The effect of the water absorption into the polymer system can readily be seen in the figure as the glass transition greatly decreases. From this figure one can also infer the relative duration of the transition region. The difference between the  $T_g$  and  $T_{on}$  of the 100% tBA over the 50/50% tBA-2HEMA is an indication of a steep transition region vs. a more gradual transition, and can be compared to **Figure 6**. A steep transition is favored.

### 6.3 Mechanical Properties of Final Network

Once the ternary network was customized for (1) glass transition temperature and (2) water absorption, a detailed inquiry was further made into the DMA and mechanical properties of the material.

A representative result from DMA testing of the final network can be seen below in **Figure 8 (a)**. Storage modulus is plotted on the left-hand axis, while the materials Tan delta is plotted on the right, both as a function of temperature. A five order of magnitude change in the materials storage modulus over the temperature range can be seen and is indicative of a transition of the material from its glassy region at lower temperatures to its rubbery region at the higher temperatures.

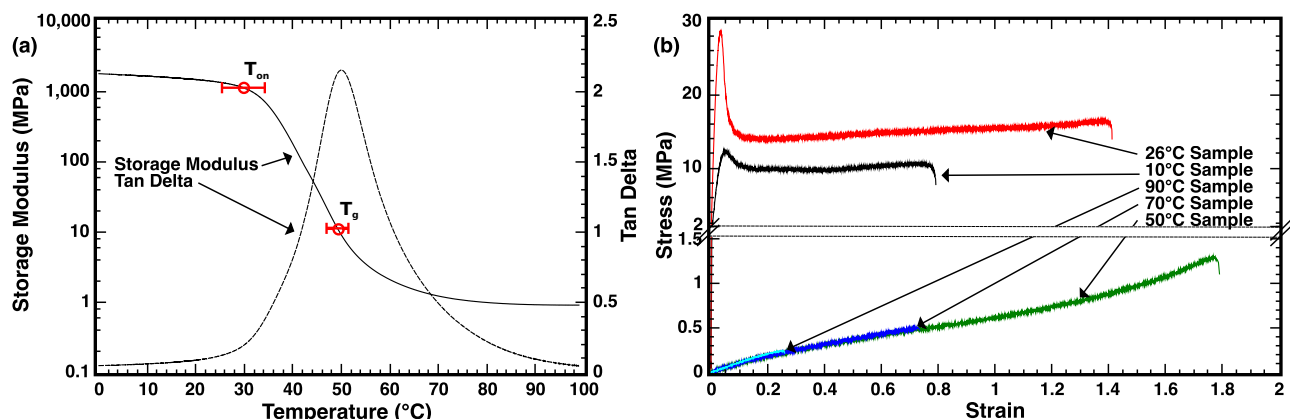


**Figure 8:** (a) Representative DMA curve of final ternary network along with the average  $T_{on}$ ,  $T_g$  of the tests. (b) Tensile stress strain behavior as a function of temperatures tested over the glass transition region.

Additional test results found an onset temperature of  $29.8 \pm 4.4^\circ\text{C}$  and a glass transition temperature of  $49.2 \pm 2.2^\circ\text{C}$ , which are represented on the storage modulus curve in the figure. Note the modulus at five different temperatures that are used in tensile tests displayed in **Figure 8 (b)**. These points are tabulated in **Table 1** highlighting the orders of magnitude decrease in stiffness over the transition region.

**Table 1:** Average sample storage moduli, ultimate tensile strength, and strain to failure at various temperatures.

	Storage Modulus (MPa)	Ultimate Tensile Strength (MPa)	Strain to Failure	Toughness ( $\text{kJ/m}^3$ )
10 °C	$1405 \pm 437$	$14.22 \pm 2.80$	$0.600 \pm 0.182$	$4,830 \pm 3,120$
26 °C	$916 \pm 386$	$19.65 \pm 6.95$	$1.405 \pm 0.084$	$17,240 \pm 5,220$
50 °C	$7.13 \pm 3.08$	$0.934 \pm 0.469$	$1.607 \pm 0.267$	$688 \pm 430$
70 °C	$1.130 \pm 0.150$	$0.480 \pm 0.063$	$0.872 \pm 0.162$	$200 \pm 52.7$
90 °C	$0.810 \pm 0.350$	$0.139 \pm 0.094$	$0.1749 \pm 0.0781$	$15.85 \pm 16.30$

The five temperature regions mentioned above were examined due to their location in the glassy-to-rubbery transition region. First well into the glassy region at  $10^\circ\text{C}$ , next at room temperature of  $\sim 26^\circ\text{C}$  - close to the onset temperature, then at the glass transition temperature of  $50^\circ\text{C}$ , and rounded off at  $70^\circ\text{C}$  and  $90^\circ\text{C}$  which have transitioned fully into the rubbery region of the material.

As the material transitions from its glassy to rubbery regime, its mechanical properties are also expected to change. These transitions can be seen in the representative stress-strain curves for each of the five temperatures displayed in **Figure 8 (b)**. Results of strain to failure and ultimate tensile strength are additionally tabulated as a function of temperature in **Table 1**.

In **Figure 8 (b)** as well as **Table 1** note the large change in the material's mechanical behavior as temperature transitions from high to low both in ductility and ultimate strength, as well as overall behavior. There is a fundamental change in characteristic behavior between the  $50^\circ\text{C}$  and  $26^\circ\text{C}$ , the glass and onset temperatures respectively.

## 6.4 Molding Techniques

A large emphasis in this project was placed into development of an adequate soft molding technique, as the uncured acrylate system was found to absorb, at least to some degree, into a variety of silicone molding materials, including Silastic® 7-4860 silicone elastomer, Sylgard® 184 silicone elastomer, and Xiameter® RTV-4251-S2 silicone mold making rubber. All three of the silicones selected had various different advantages and disadvantages, and through experimentation the best solution was found involving a multi-step processes starting with a Delrin custom machined negatives of the structured surface (or master mold), Silastic elastomer, and finally followed by a Xiameter mold making rubber.

The soft molding technique can be better understood through observing **Figure 9**, where the six steps are shown from left to right. The first frame of the Figure, (a), displays a model of the prepared Delrin mold. Represented in frame (b) is Silastic- colored blue in the figure - which is supplied in extremely viscous two part base constituents that are mixed in equal parts to start the chemical polymerization of the substance. Stain-to-failure tensile testing comparing Silastic and Sylgard showed a much higher material toughness in Silastic, allowing for a more robust product during positive-negative mold delamination.

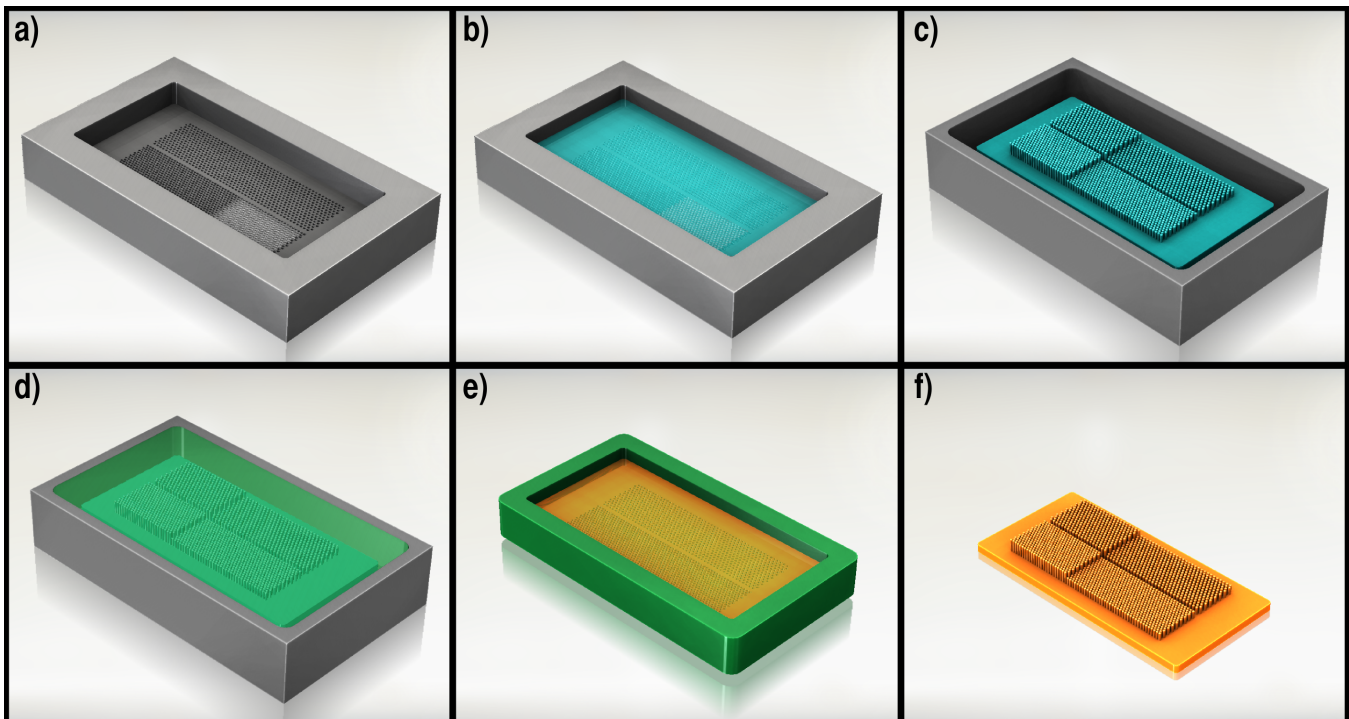


**Figure 9:** Soft molding process of acrylate structured surface. The Delrin master mold in (a) is (b) cast with Silastic creating an intermediate positive (c). After surface treatment, another silicone substance is poured and cured (d) creating a clone (e) that can be used to cure the final acrylate structure shown in (f).

As seen in frame (c), once the Silastic positive was demolded, it was placed in a custom dish that maintained the footprint of the positive, and added deeper walls that would ultimately allow for pouring the acrylate system into the Xiameter negative. Because both the Silastic and the Xiameter are silicon based materials, a release agent was necessary between the positive and negative molds. 11 mL of a Trichloro(1H,1H,2H,2H-perfluorooctyl)silane (PFOS)/Hexane solution (ratio 1:10) was placed in an open dish next to the sample and vacuum desiccated to approximately 380 Torr, sealed, and left for one day in order to be vapor deposited, creating a self assembled monolayer on the Silastic surface. The monolayer was then annealed at 150°C in an open-air furnace for one hour.

Immediately after vapor deposition of the release agent for 1 day, Xiameter was mixed in at 10:1 weight ratio of base to curing agent with a stainless stir rod and poured onto the Silastic mold and dish; represented by the green material in (d). The material was degassed and cured at 150°C for one hour. This method allowed for a good de-lamination between the Silastic positive and Xiameter negative.

With the welled Xiameter negative, the ternary acrylate network could finally be cast into the structured surface as is displayed in (e). Before casting, the polymer system was pre-cured using a 254 nm wavelength crosslinking oven for 15 minutes. The mixture was then poured in it the Xiameter mold, degassed for one minute, and photopolymerization was completed using a the 365 nm wavelength UV lamp for 15 minutes and placed in the oven at 90°C for 60 minutes. This process ultimately provided the final structured Acrylate surface seen in (f).

However, an alternative molding process involved moving directly from the Delrin master mold straight to the acrylate system. Although direct molding into the master negative was a higher risk operation with potential for permanently plugging the master mold, it proved more effective for creation of small section test samples, allowing for accurate delamination between both parts in a less time intensive process when compared to the soft molding techniques. Masters could typically be used approximately five times before deforming too much from the curing process, or being damaged with too much residual acrylate, requiring a new mold. The process described below is represented in **Figure 10**.

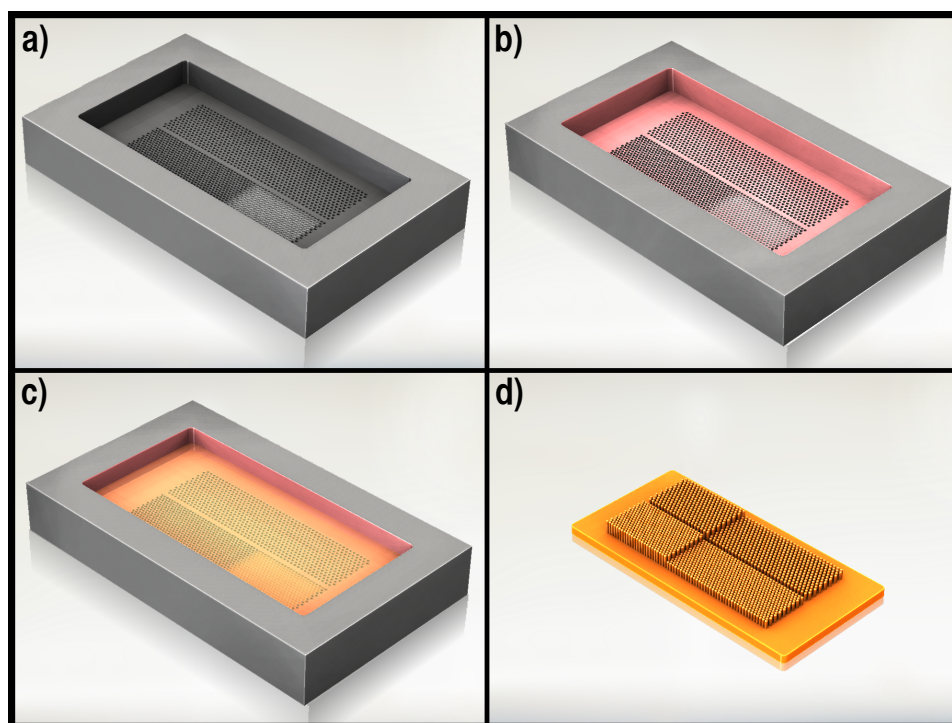


**Figure 10:** Direct molding process of acrylate structured surface. An (a) untreated Delrin mold is coated with an annealed monolayer of PFOS (b). In (c) the acrylate could be cast directly into the material and cured producing the final product (d).

To ensure the acrylate network would not adhere to the Delrin (a), molds first needed to be coated with a self-assembled film to act as a release agent, PFOS, shown in (b). A 10 mM solution of PFOS in Hexane was poured into the mold, placed in the refrigerator, and after 20 minutes, samples were removed from

the solution and rinsed heavily with Hexane to remove any loosely bonded self assembled layer. Samples were finished curing in an open-air furnace at 150°C for 60 minutes, annealing the coating. With the self-assembled coating polymerized on the mold surface, represented as the red coating in the Figure, the final ternary polymer structure could be cast in frame (c). The acrylate was first pre-cured in a 254 nm wavelength crosslinking oven for 20 minutes, placed in the mold, degassed, finished polymerizing under a 365 nm wavelength UV lamp for an additional 10 minutes, and subsequently placed in an oven at 90°C for 60 minutes. The method allowed for simple delamination from the mold at elevated temperatures. Typically a direct molding process would be improbable, as their needs to be a large difference in elastic modulus between the mold and the product, hence the usual use of soft molding. However the acrylate has the benefit of becoming rubbery upon heating to assist in removal here, working excellently on the small scales here.

### 6.5 Surface Modification

Various methods of surface treatments could be employed to alter the wettability of the surface of the acrylate, regardless of the acrylate's water absorption characteristics. Ultimately, this could allow for different surface characteristics at various points in the structured pillared surface, creating a switchable properties. Three methods were investigated including Polydopamine coating (PDOPA), Trichloro(1H,1H,2H,2H-perfluorooctyl)silane coating (PFOS), and dip coating of Sylgard 184 silicone elastomer (PDMS).

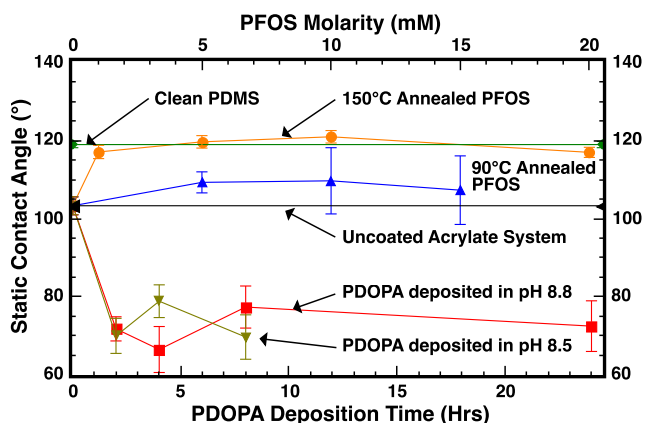


**Figure 11:** Contact angles of surface treatments applied to the final acrylate system.

**Figure 11** displays the mean and one standard deviation of static contact angle results of PDOPA and PFOS surface coatings on flat sheets of the final acrylate system after soaking in ultra-pure water for 24 hours from a sample size of five to seven. These can be compared to results of pure PDMS and the final acrylate system's static contact angles with no variation in their material properties. PDOPA varied both deposition time as well as the pH of the deposition medium, and corresponds to the bottom axis. PFOS observations were made altering the solution concentration and annealing temperature, corresponding to the top axis. Note all PDOPA and PFOS results start with the uncoated Acrylate material contact angle of  $103.3 \pm 2.3^\circ$  that was to be modified.

From the figure, it appears there is little difference between a deposition pH of 8.5 and 8.8 in the PDOPA coating process, though there is a large amount of variation in the initial process around 4 to 8 hours. Average results at 24 hours for a pH of 8.5 are  $72.4 \pm 6.5^\circ$ , and are expected to be similar for a pH of 8.8.

The two curves of PFOS, annealed at different temperatures, follow the same trend being slightly optimized between a 5 and 10 mM deposition concentration, while decreasing a small amount at 20 mM. The importance of annealing temperature is also highlighted in the curves as the contact angles of a 10 mM solution increases from  $109.7 \pm 8.5^\circ$  to  $121.0 \pm 1.6^\circ$  with an increase in temperature from  $90^\circ\text{C}$  to  $150^\circ\text{C}$ . Therefore, PFOS can be considered similar to the pure PDMS sheets of  $119.0 \pm 0.8^\circ$ . Results of pure PDMS complement results from Jin et al. static contact angles at  $113^\circ$  [5].

## 6.6 Combined Structured Surface

With investigation of all facets of the research complete, the structure surface could finally be combined, showing a proof-of-concept design. Pillared surface were first subjected to PDOPA treatment polymerized in a pH solution of 8.5 for 24 hours, leaving a mainly hydrophilic surface coating. The pillar tops were then either dipped in PDMS and cured, producing a hydrophobic flanged top, or placed in a PFOS bath, creating a self-assembled monolayer that was also very highly hydrophobic. Qualitative results with close ups of the final structured surface coated with various surface treatments in contact with water droplets are displayed in **Figure 12**. For the images, samples were presoaked, and subsequently dabbed to free surface water before placing a water drop on top.

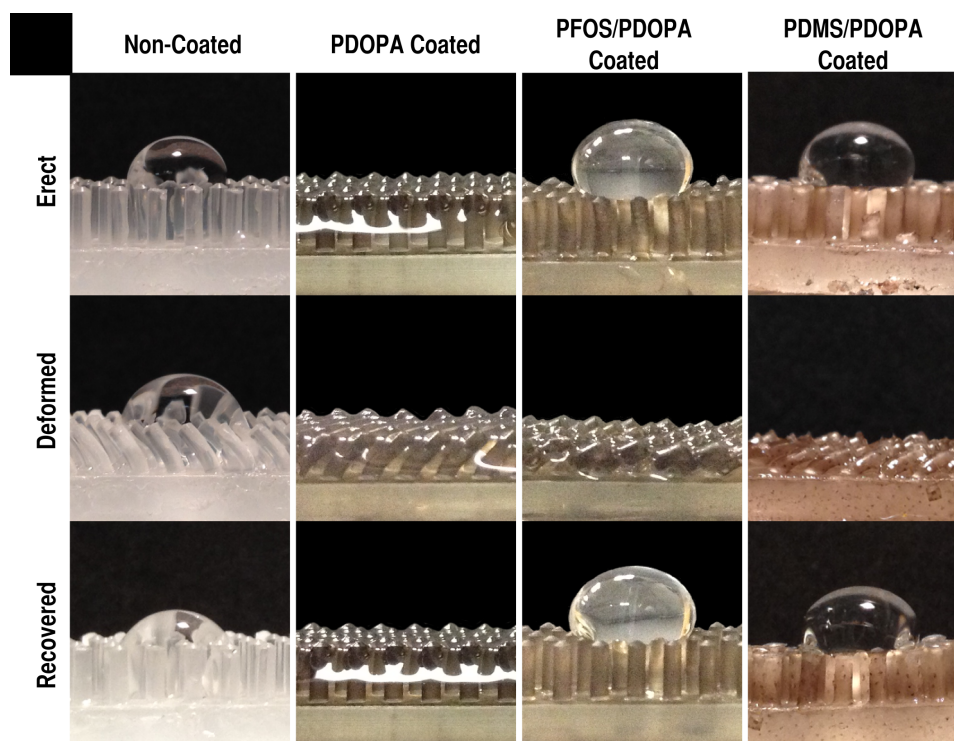


**Figure 12:** Qualitative results of water droplets in contact with structured acrylate system with various surface coatings (columns) in erect, deformed, and recovered conditions.

Columns from right to left include the non-coated structured acrylate system, PDOPA coated throughout, PDOPA coated with PFOS topping, and PDOPA coated with flanged PDMS pillar tops. The first row displays the material in the original un-deformed state, the second in the deformed state, and the third in the recovered state. Results qualitatively show the switchable hydrophobic effects, when using a

combination of the pillar structure with surface treatments. Noting the first column, it is important, at least on the size scale here, that surface treatments are key for the switchable hydrophobic effect. The last two columns exemplify this characteristic, where the water (and any type of fouling material) is exposed to the hydrophobic tops, it displays hydrophobic behavior, but when relaxed, the pillars expose the hydrophilic surface, dispersing the water. This can then be returned to its original state.

## 7 Discussion / Significance:

A proof-of-concept, switchable hydrophobic, structured surface was created in this research, with an ultimate targeted application acting as assistance to antifouling in pressure driven water treatment membranes. This was done through a multi-tiered design using a patterned shape memory polymer with selectively treated surface locations, inducing a hydrophobic or hydrophilic effect.

A majority of the research presented here focused on investigation and design of a custom tailored shape memory polymer that could be cast into a structured surface. The final composition of this ternary acrylate polymer consisted of 94.5/ 5.0/ 0.5 wt.% linear building mixture of 9:1 tBA:2HEMA, PEGDMA550, and DMPA, or a final relative weight percentage of each constituent overall of 85.05/ 9.45/ 5.00/ 0.50 wt.% tBA, 2HEMA, DEGDMA, and DMPA. The polymer was optimized for good shape memory properties in a targeted temperature range, water absorption characteristics, and applicable thermo-mechanical properties. Final glass transition and onset temperatures were  $49.2\pm 2.2^{\circ}\text{C}$  and  $29.8\pm 4.4^{\circ}\text{C}$  respectively.

The second stage focused on developing the basis for a structured surface. Emphasis was placed on research-scale manufacturing processes to cast patterned structured surfaces as well as application of hydrophilic and hydrophobic surface treatments, and how to selectively locate them on the cast surface. A manufacturing method for the surfaces at the research scale was not immediately apparent, taking a large amount of research, though in the end two processes emerged. This included a soft molding process as well as a direct molding process, which both had their advantages and disadvantages depending on the requirements of the final product.

Thirdly, this project developed a reliable method of altering surface properties especially along the cast pillar surface through the use of PFOS, PDMS, and PDOPA. The major advantage to altering surface characteristics is that the underlying structure can remain the same, while locally the material can be made hydrophobic or hydrophilic. It is through the combination of the materials geometry, as well as the surface characteristics that we can see the stark change in the apparent hydrophobicity of the surface, as seen in the final figure, **Figure 12**.

Through this funding, significant progress was made into the novel surface, laying the groundwork that can be built upon with additional work. We have shown through proof-of-concept the framework for a switchable surface including a custom designed acrylate system, appropriate molding techniques, and application of surface treatments that can easily be spatially modified. Future work can therefore build upon this design, taking it to a smaller scale, optimizing the geometrical patterning and direct fouling testing. However, the steps taken here are significant strides towards a surface that will, in the future, aid in membrane filtration processes.

## 8 Project Publications:

### 8.1 Thesis

C. M. Laursen, “Proof-of-concept switchable hydrophobic/hydrophilic patterned surfaces from thermo-mechanically tailored acrylate systems,” M.S. thesis, Dept. Mech. Eng., Univ. of Wyo., Laramie, WY, 2014.

### 8.2 Publications

A paper is being prepared for submission to *Surface and Coatings Technology*, summer 2015.

## 9 Student Support and Training:

*Graduate:* Christopher M. Laursen, M.S. Mechanical Engineering 2014  
Anthony J. Hoyt, M.S. Mechanical Engineering 2015

*Undergraduate:* Samuel R. Gates, B.S. Mechanical Engineering 2014  
Aidan H. McDonald, B.S. Mechanical Engineering exp. 2016

## 10 References:

[1] M. M. Benjamin and D. F. Lawler, *Water Quality Engineering: Physical/Chemical Treatment Processes*. Hoboken: Wiley, 2013.

[2] T. Asano, F. L. Burton, H. Leverenz, R. Tsuchihashi, and G. Tchobanoglous, *Water Reuse Issues, Technologies, and Applications*. McGraw-Hill, 2007.

[3] J. Mallevalle, P. Odendaal, and M. Wiesner, *The Emergence of Membranes in Water and Wastewater Treatment*, in *Water Treatment Membrane Processes*. McGraw-Hill, 1996.

[4] S. J. Duranceau, “The future of membranes,” *Journal American Water Works Association*, vol. 92, no. 2, pp. 70–71, 2000.

[5] M. Jin, X. Feng, J. Xi, J. Zhai, K. Cho, L. Feng, and L. Jiang, “Super-hydrophobic PDMS surface with ultra-low adhesive force,” *Macromolecular Rapid Communications*, vol. 26, pp. 1805–1809, Nov 14 2005.